

Article

Supported Ni Catalyst for Liquid Phase Hydrogenation of Adiponitrile to 6-Aminocapronitrile and Hexamethylenediamine

Chengqiang Wang ¹, Zekun Jia ¹, Bin Zhen ^{1,2} and Minghan Han ^{1,*}

¹ Department of Chemical Engineering, Tsinghua University, Beijing 100084, China; thuwcq@163.com (C.W.); jiazekun1991@163.com (Z.J.); zhenbin@tjut.edu.cn (B.Z.)

² College of Chemistry and Chemical Engineering, Tianjin University of Technology, Tianjin 300384, China

* Correspondence: hanmh@tsinghua.edu.cn; Tel.: +86-10-6278-1469

Received: 25 November 2017; Accepted: 30 December 2017; Published: 4 January 2018

Abstract: Supported Ni catalysts prepared under different conditions, for liquid phase hydrogenation of adiponitrile (ADN) to 6-aminocapronitrile (ACN) and hexamethylenediamine (HMD), were investigated. The highly reactive imine intermediate can form condensation byproducts with primary amine products (ACN and HMD), which decreased the yield coefficient of primary amines. The catalysts support, condition of catalyst preparation and dosage of additive were studied to improve the yield. A highly dispersed Ni/SiO₂ catalyst prepared by the direct reduction of Ni(NO₃)₂/SiO₂ suppressed the condensation reactions by promoting the hydrogenation of adsorbed imines, and it gave the improved hydrogenation activity of 0.63 mol·kg_{cat}⁻¹·min⁻¹ and primary amine selectivity of 94% when NaOH was added into the reactor.

Keywords: supported Ni catalyst; adiponitrile hydrogenation; 6-aminocapronitrile; hexamethylenediamine

1. Introduction

The hydrogenation of ADN to ACN and HMD is an important industrial process [1–4], which is mainly catalyzed by Raney Ni catalysts [5,6]. Although the skeleton structure of Raney Ni catalysts favors a high catalytic activity, it causes low mechanical strength and bad regeneration capability. In addition, a safety hazard also exists as the Raney Ni catalysts are flammable when exposed to air. Due to these drawbacks, many researchers have been working on developing supported Ni catalysts to replace Raney Ni. The use of a supported Ni catalyst can dramatically reduce the cost of the catalyst, making the process easy to operate and improving the safety of the hydrogenation reaction. The main challenge is that so far, the supported Ni catalysts are inferior in terms of catalytic activity and primary amine selectivity [7,8].

The reaction scheme for the hydrogenation of ADN is given in Figure 1 [9–11]. ADN is hydrogenated to ACN and then to HMD. During the sequential hydrogenation, a highly reactive imine intermediate is formed, which has a strong tendency towards intermolecular condensation with the primary amine products (ACN and HMD) and intramolecular cyclization to undesired condensation byproducts and hexamethyleneimine (HMI). The formation of the primary amines has to compete with these side reactions. From the chemistry, it can be seen that increasing the hydrogenation activity of the catalyst would be an effective way to suppress the byproducts.

In this work, supported Ni catalysts were studied from several aspects, such as the type of support, conditions of catalyst preparation and dosage of additive, in order to increase the yield of primary amines. A highly dispersed Ni/SiO₂ catalyst prepared by the direct reduction of a Ni(NO₃)₂ precursor [12] was found able to promote the hydrogenation of the imine intermediate so that its performance was close to that of Raney Ni.

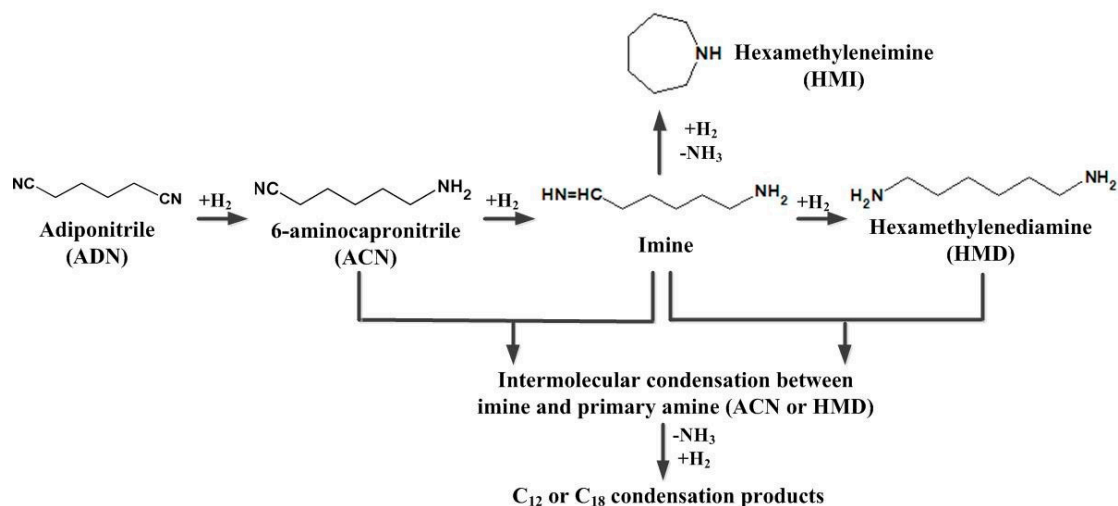


Figure 1. Mechanism of ADN hydrogenation.

2. Results and Discussion

2.1. Catalyst Support

Since the catalyst support has an important influence on the catalytic performance, the effect of different supports was investigated. Many oxides can be used as the support, among which Al_2O_3 and SiO_2 are the most widely used. The characterization result of the specific surface area and pore structure of the Al_2O_3 , SiO_2 and $\text{Ni}/\text{Al}_2\text{O}_3$, Ni/SiO_2 used are shown in Table 1. The evaluation result in Table 2 showed the Ni/SiO_2 was better than $\text{Ni}/\text{Al}_2\text{O}_3$ in terms of the selectivity of primary amines and condensation byproducts.

Table 1. Specific surface area and pore structure of the supports and the catalysts.

Sample	Specific Surface Area/ $\text{m}^2\cdot\text{g}^{-1}$	Pore Volume/ $\text{cm}^3\cdot\text{g}^{-1}$	Average Pore Size/nm
Al_2O_3	242	0.64	9.9
$\text{Ni}/\text{Al}_2\text{O}_3$	175	0.41	9.5
SiO_2	245	0.94	17.8
Ni/SiO_2	190	0.72	17.4

Table 2. Evaluation reaction result of Ni/SiO_2 and $\text{Ni}/\text{Al}_2\text{O}_3$.

Catalysts	Catalytic Activity/ $\text{mol}\cdot\text{kg}_{\text{cat}}^{-1}\cdot\text{min}^{-1}$	Selectivity/%			
		ACN	HMD	HMI	Condensation Byproducts
Ni/SiO_2	0.25	50	4	9	37
$\text{Ni}/\text{Al}_2\text{O}_3$	0.29	43	4	8	45

Using the bifunctional mechanism [13], it is believed that in a nitrile hydrogenation system, the hydrogenation reactions are catalyzed by metal sites while condensation reactions are catalyzed by acid sites. This would indicate that the acidic properties of the support are crucial to the catalytic performance. A stronger acidity favors the conversion of nitrile but decreases the selectivity to primary amines. The NH_3 -TPD data for Al_2O_3 and SiO_2 and their corresponding catalysts are presented in Figure 2a. Al_2O_3 has a large NH_3 desorption peak in the temperature range from 100 to 500 °C while SiO_2 does not. After the introduction of the Ni, $\text{Ni}/\text{Al}_2\text{O}_3$ still showed an obvious NH_3 desorption peak in contrast to Ni/SiO_2 as shown in Figure 2b. The acid sites can absorb imine intermediate and primary amine and cause them to react with each other so that condensation products are produced, which lead to the decreased selectivity of the target products.

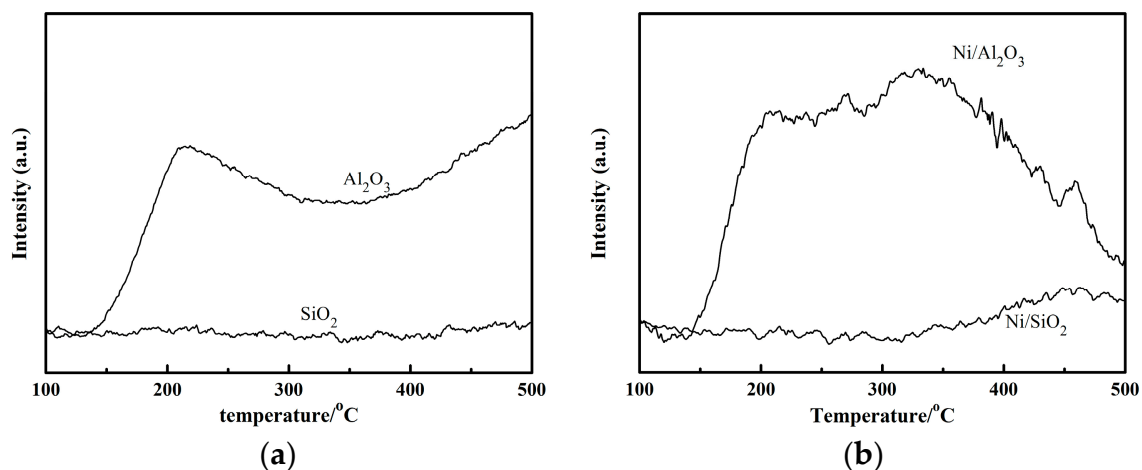


Figure 2. NH_3 -TPD of (a) Supports and (b) Catalysts.

Therefore, SiO_2 is the more suitable support for the hydrogenation of ADN to ACN and HMD, and SiO_2 was used as the support in the following study.

2.2. Direct Reduction Method

The supported Ni catalyst was prepared by the wetness incipient impregnation method, which consists of three steps: impregnation, calcination and reduction. After calcination and reduction, the $\text{Ni}(\text{NO}_3)_2$ loaded on the supports became metal particles with catalytic activity. The calcination and reduction are key steps and have important influence on the catalytic performance.

Table 3 shows mean particle sizes of Ni estimated by the two independent methods, TEM and XRD analysis [14]. Figure 3 showed the TEM images of two catalysts. The particle size of nickel on the $\text{Ni}_{\text{DR}}/\text{SiO}_2$ is around 7 nm, while that on the $\text{Ni}_{\text{CR}}/\text{SiO}_2$ is much larger. XRD analysis results of the catalysts show the similar information, 6.4 and 17.7 nm, respectively.

Table 3. Ni particle size of $\text{Ni}_{\text{CR}}/\text{SiO}_2$ and $\text{Ni}_{\text{DR}}/\text{SiO}_2$ from TEM and XRD analysis.

Sample	Ni Particle Size(a) ¹ /nm	Ni Particle Size(b) ² /nm
$\text{Ni}_{\text{CR}}/\text{SiO}_2$	19	17.7
$\text{Ni}_{\text{DR}}/\text{SiO}_2$	7	6.4

¹ Estimated by TEM analysis. ² Calculated by XRD analysis according to Scherrer equation.

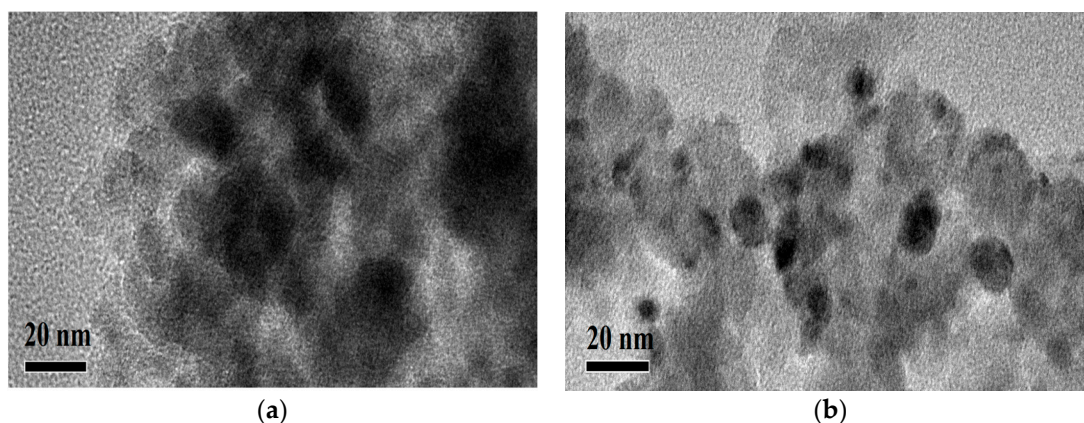


Figure 3. TEM images of (a) $\text{Ni}_{\text{CR}}/\text{SiO}_2$ and (b) $\text{Ni}_{\text{DR}}/\text{SiO}_2$.

The H₂ uptake was 76.2 μmol/g by Ni_{DR}/SiO₂ while that by Ni_{CR}/SiO₂ was 15.4 μmol/g, corresponding to the active nickel areas of 30.0 and 6.0 m²/g [15]. We can conclude that Ni_{DR}/SiO₂ had a superior Ni dispersion of 4.50% while that of Ni_{CR}/SiO₂ is 0.90%, which is in accordance with the TEM and the XRD analysis. Ni(NO₃)₂/SiO₂ catalyst precursor would be totally reduced at 700 °C from H₂-TPR profiles. The H₂-chemisorption data showed the H₂ adsorption capacity of a catalyst partially reduced at 450 °C. This means that H₂-chemisorption data here cannot be used to calculate the mean particle size accurately.

Figure 4 showed the XRD patterns of the catalysts. The characteristic diffraction peaks of NiO in Ni_C/SiO₂ are obvious, which indicated that the nickel mainly existed in the form of nickel oxide. After the reduction in H₂, Ni_{CR}/SiO₂ showed a very sharp Ni peak while Ni_{DR}/SiO₂ showed both NiO and Ni diffraction peaks. Louis et al. [16] have studied supported Ni catalyst and found existence of nickel phyllosilicates, which were located at the surface of catalyst precursor after nickel nitrate impregnated onto silica. The nickel phyllosilicates act as anchoring sites for metallic Ni particles and suppress the formation of large Ni particles. However, calcination before reduction leads to the formation of larger metal particles and to their aggregation. This is probably due to the partial decomposition of nickel phyllosilicates during calcination, the breaking of the anchoring sites for impregnated nickel, which favors nickel migration. Direct reduction of Ni(NO₃)₂/SiO₂ was a moderate reduction process, which sacrificed the reduction degree but gave a superior Ni dispersion.

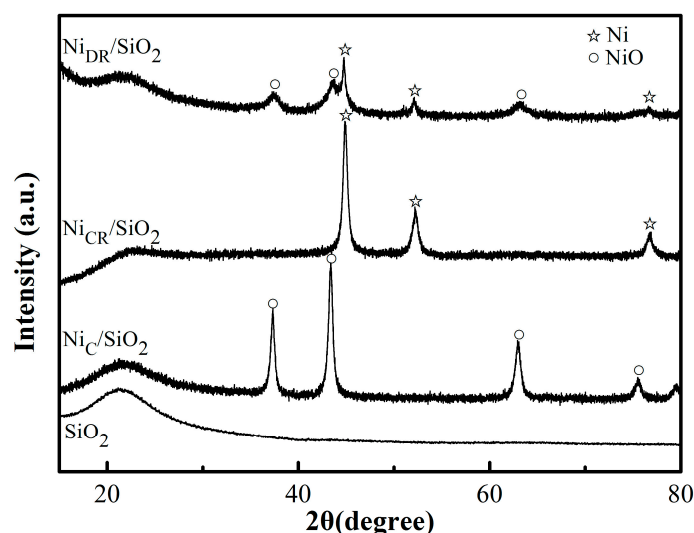


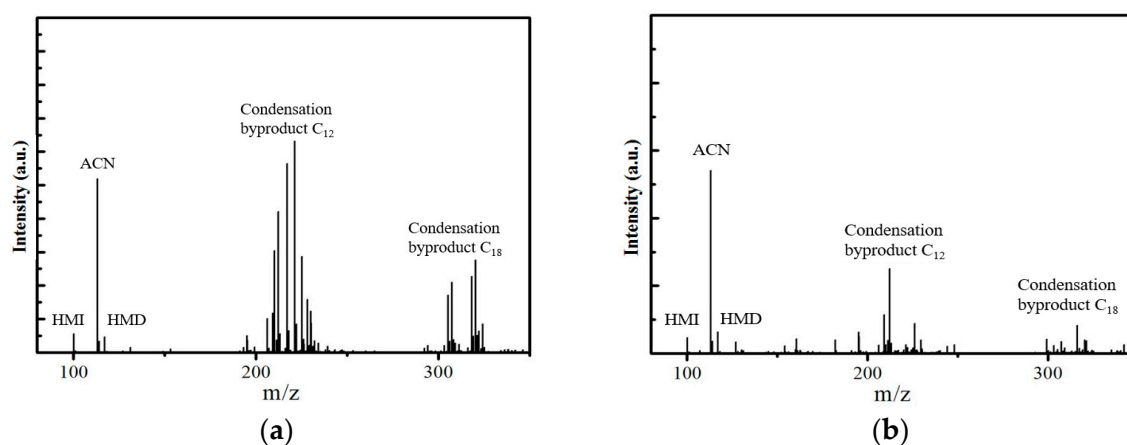
Figure 4. XRD pattern of SiO₂, Ni_C/SiO₂, Ni_{CR}/SiO₂ and Ni_{DR}/SiO₂.

As described above, the two catalysts prepared by the different methods had different microstructures, which probably caused their catalytic performance for hydrogenation of ADN to be different. Table 4 shows the evaluation result of the catalysts. Ni_{DR}/SiO₂ exhibited a better hydrogenation activity of 0.56 mol·kg_{cat}⁻¹·min⁻¹ compared to Ni_{CR}/SiO₂ with 0.25 mol·kg_{cat}⁻¹·min⁻¹. The selectivity to the primary amine products over Ni_{DR}/SiO₂ was higher than that over Ni_{CR}/SiO₂, which, respectively, were 79% and 54%. Meanwhile, the selectivity to condensation byproducts were inhibited over Ni_{DR}/SiO₂, which decreased from 37% to 3%. In the sequential reaction, shown in Figure 1, the highly reactive imine intermediate can further react along three pathways: further hydrogenation, intramolecular condensation to HMI, and intermolecular to condensation byproducts. The three pathways are parallel, that is, the formation of primary amine competes with the side reactions. Ni_{DR}/SiO₂ exhibited a superior hydrogenation activity, which promoted the hydrogenation and improved the selectivity to ACN and HMD.

Table 4. Evaluation reaction result of Ni_{CR}/SiO₂ and Ni_{DR}/SiO₂.

Catalysts	Catalytic Activity/Mol·kg _{cat} ⁻¹ ·min ⁻¹	Selectivity/%			
		ACN	HMD	HMI	Condensation Byproducts
Ni _{CR} /SiO ₂	0.25	50	4	9	37
Ni _{DR} /SiO ₂	0.50	66	13	18	3

The condensation byproducts were secondary and tertiary amines with a high molecular weight which were not eluted and cannot be detected in the GC analysis. The product mixture was analyzed by a mass spectrometer to confirm the existence of condensation byproducts. The result is shown in Figure 5. The mass to charge ratio of protonated HMI, ACN and HMD are, respectively, $m/z = 100$, 113, 117. The peaks of $m/z = 200\sim 300$ indicated the formation of C₁₂ and C₁₈ oligomers. These showed clearly that the condensation byproducts from Ni_{DR}/SiO₂ was decreased, which verified the GC evaluation result.

**Figure 5.** Mass spectra of (a) Ni_{CR}/SiO₂ and (b) Ni_{DR}/SiO₂.

Ni_{DR}/SiO₂ had a higher H₂ adsorption capacity from H₂ uptake result, which would indicate that amines and imine intermediates are more abundantly adsorbed on Ni_{DR}/SiO₂. The C atoms of imines were subjected to nucleophilic attack by N atoms of the amines [17], leading to the formation of a secondary imine which can be further hydrogenated to HMI. Ni_{DR}/SiO₂ was more selective for intramolecular side reaction. As seen in Table 4, the selectivity to HMI over Ni_{CR}/SiO₂ was 9% while that over Ni_{DR}/SiO₂ was 18%. From this point, further developing of the supported Ni catalyst prepared by the direct reduction method is still necessary. The conditions of catalyst preparation and reaction conditions have to be optimized to inhibit the formation of HMI and improve the selectivity to primary amines.

2.3. Reduction Temperature

The microstructure of supported Ni catalyst prepared by direct reduction method is affected by reduction temperature significantly. The TEM images of catalysts reduced at different temperature are shown in Figure 6. The mean particle sizes of Ni became larger with the increase of reduction temperature obviously.

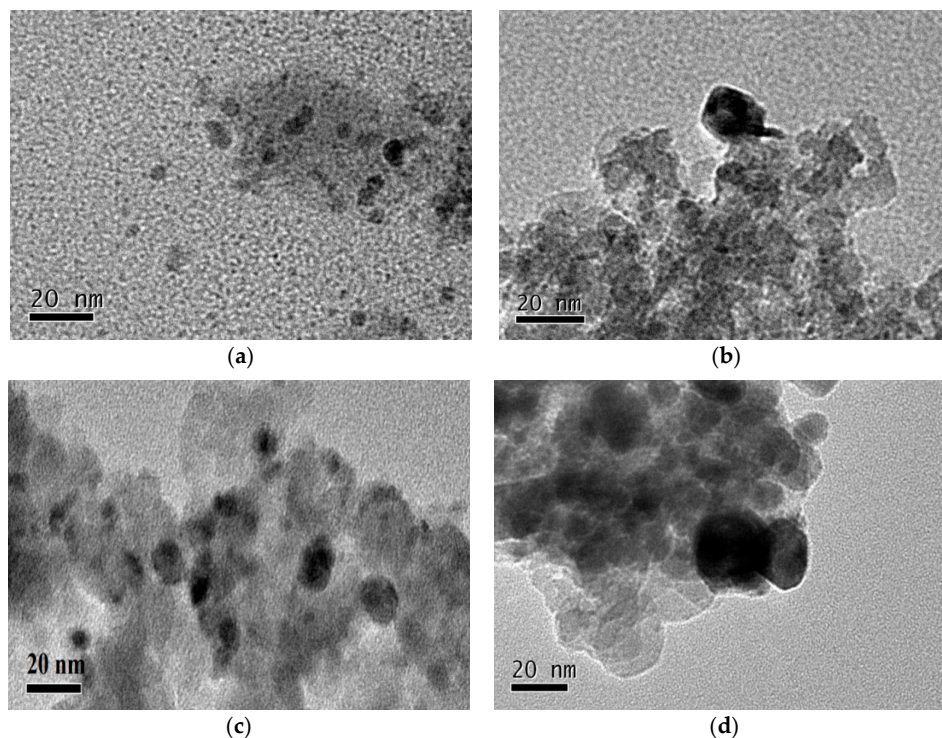


Figure 6. TEM images of the catalysts reduced at different temperatures: (a) 350 °C; (b) 400 °C; (c) 450 °C; (d) 500 °C.

The H₂-TPR profiles of Ni(NO₃)₂/SiO₂ were given in Figure 7. The TPR profiles of the impregnated catalysts, performed without any previous calcination, exhibit three peaks of hydrogen consumption at 300, 400, and about 550 °C, attributed to the decomposition of nickel nitrate into NiO, the reduction of NiO and the reduction of nickel phyllosilicates. After TPR up to 700 °C, the nickel is totally reduced. Before complete reduction, the nickel phyllosilicates are probably located at the interface between silica and the remaining nickel, for which they act as anchoring sites. During TPR, after nitrate decomposition, the NiO particles located on the phyllosilicates are reduced into Ni⁰ at 400 °C without any migration. Between 400 and 700 °C, the increase in metal particle size is due not only to NiO migration induced by thermal effect but also to the reduction of the phyllosilicates by the weakening of the anchoring strength.

The H₂-TPR profiles of Ni(NO₃)₂/SiO₂ are in accordance with the TEM analysis of the four catalysts reduced at 350, 400, 450 and 500 °C, respectively.

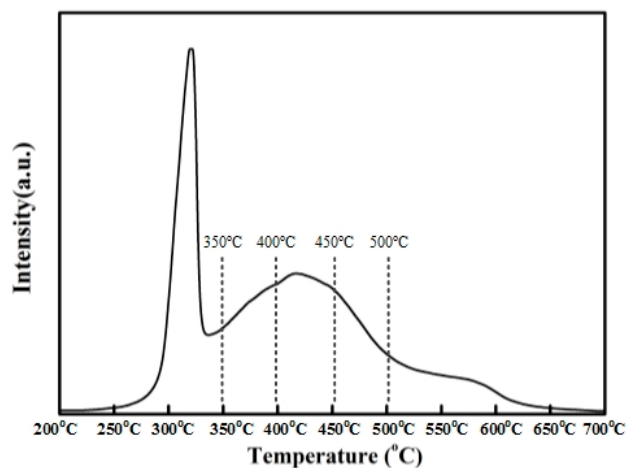


Figure 7. H₂-TPR of catalyst precursors.

Figure 8 presents the evaluation result of the four catalysts. The catalytic activity first decreased and then increased with the increase of reduction temperature, which can be explained by the reduction degree and Ni dispersion. With the increase of reduction temperature, the reduction degree of the catalysts became higher while the Ni dispersion became lower because the nickel phyllosilicates were gradually decomposed. Ni/SiO₂ reduced at 350 °C had a high hydrogenation activity because of its high Ni dispersion. When the reduction temperature was increased to 400 °C and 450 °C, the migration and aggregation of Ni particles led to a lower metallic Ni dispersion, which caused the catalytic activity decrease. Although the Ni dispersion of Ni/SiO₂ reduced at 500 °C became even lower, the catalytic activity became higher because of its higher reduction degree. In conclusion, Ni dispersion was the key factor to affect the catalytic activity for the reduction temperature range from 350 °C to 450 °C while the reduction degree was the key factor in the temperature range from 450 °C to 500 °C, which explained the variation of catalytic activity.

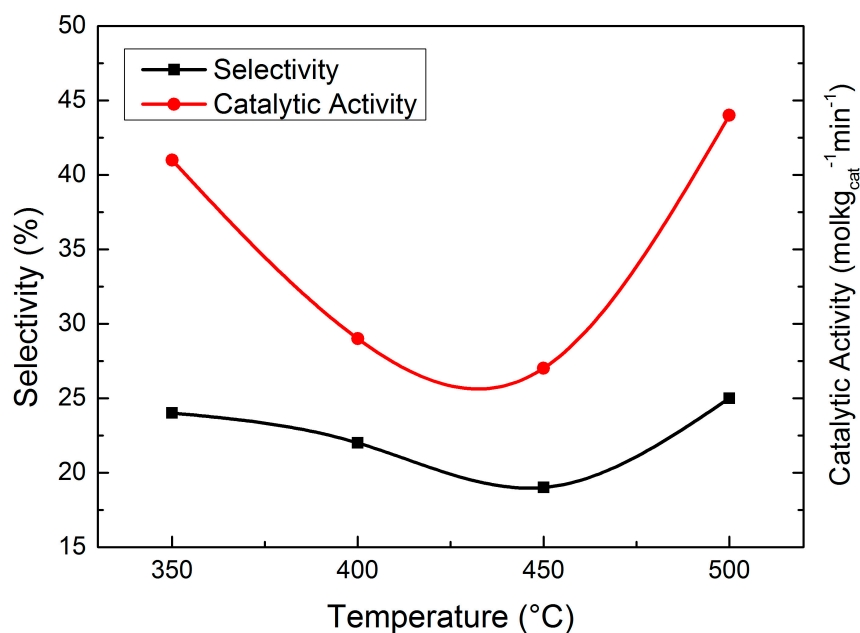


Figure 8. Evaluation result of catalysts reduced at different temperatures.

450 °C was considered the optimum temperature for the reduction when both catalytic activity and selectivity to HMI were taken into account.

2.4. Additive

Most of the side reactions are deamination reactions as shown in Figure 1. Thermodynamically, adding an alkaline substance as additive to the liquid reaction system would benefit the catalytic activity and selectivity to primary amines [5,18]. In ADN hydrogenation, H₂ and nitrile adsorbed on metallic Ni first and then they reacted with each other to imine intermediates and amines. Imines and amines desorbed from the catalyst with difficulty [19], which would not only suppress the following hydrogenation of nitriles, but also promote the condensation side reactions. The addition of an alkaline substance increases the electron density of metallic Ni on the catalyst surface, which would benefit the desorption of imine and amine [20].

NaOH was chosen as an additive to improve the Ni_{DR}/SiO₂ catalyst. The evaluation result is presented in Figure 9 and Table 5. The mass ratio NaOH/Ni was used as the independent variable. With NaOH/Ni increasing, the catalytic activity rose from 0.39 mol·kg_{cat}⁻¹·min⁻¹ to 0.63 mol·kg_{cat}⁻¹·min⁻¹ and the selectivity to condensation byproducts decreased from 12% to 1% while that to HMI decreased from 21% to 5%. When the NaOH/Ni was raised to 0.5, the primary

selectivity was as high as 94%. Clearly, the effect of NaOH on the catalytic activity and product selectivity was positive.

Table 5. Evaluation reaction result of the catalysts with different NaOH/Ni mass ratio.

NaOH/Ni	Catalytic Activity/mol·kg _{cat} ⁻¹ ·min ⁻¹	Selectivity/%			
		ACN	HMD	HMI	Condensation Byproducts
0	0.39	55	12	21	12
0.1	0.50	66	13	18	3
0.3	0.56	70	21	7	2
0.5	0.63	70	24	5	1

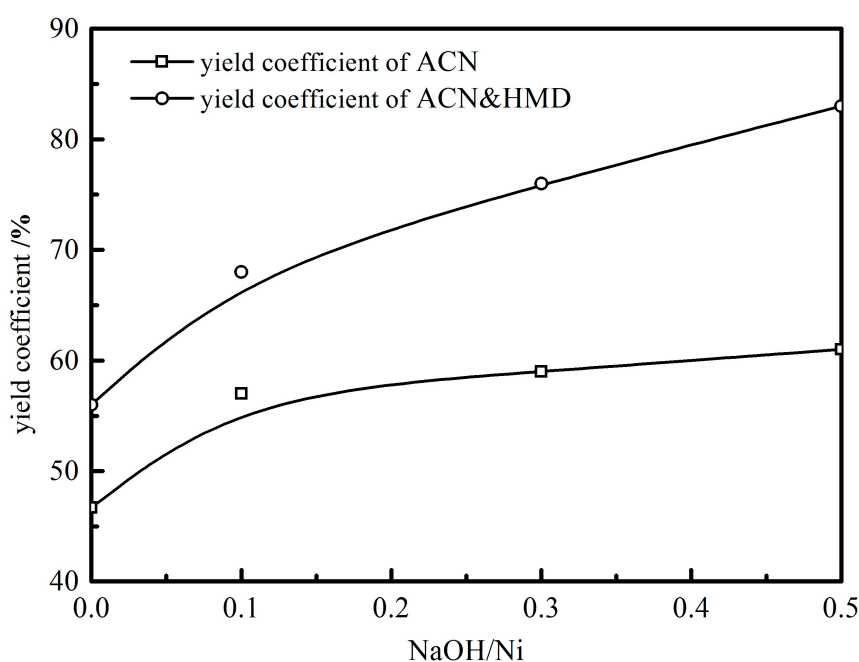


Figure 9. Evaluation result of catalysts with the use of different NaOH/Ni ratios.

The addition of NaOH improved the hydrogenation activity and improved the target products selectivity significantly. After the introduction of NaOH, the performance of Ni_{DR}/SiO₂, reduced at 450 °C, is as excellent as Raney Ni, which is presented in Table 6.

Table 6. Evaluation reaction result of the Ni_{DR}/SiO₂ and Raney Ni.

Catalysts	Catalytic Activity/mol·kg _{cat} ⁻¹ ·min ⁻¹	Selectivity/%			
		ACN	HMD	HMI	Condensation Byproducts
Raney Ni	0.61	78	17	1	4
Ni _{DR} /SiO ₂	0.63	70	24	5	1

3. Materials and Methods

3.1. Catalyst Preparation

The supported Ni catalysts were prepared by incipient wetness impregnation, which included three steps: impregnation, calcination and reduction. Ni/SiO₂ catalyst prepared by the direct reduction (DR) of Ni(NO₃)₂/SiO₂ in H₂ was denoted as Ni_{DR}/SiO₂. For comparison, another catalyst prepared by calcination and reduction (CR) was denoted as Ni_{CR}/SiO₂. They were prepared as follows. The loading amount of nickel was 20 wt.%.

$\text{Ni}_{\text{DR}}/\text{SiO}_2$: First, SiO_2 (Alfa Aesar, Haverhill, MA, USA) was soaked in an aqueous solution of $\text{Ni}(\text{NO}_3)_2$ (98%, Alfa Aesar) at room temperature. Then, the mixture was treated with ultrasonic waves for 2 h and dried at 80 °C for 12 h. Finally, the catalyst precursor was reduced in H_2 flow at 450 °C for 8 h.

$\text{Ni}_{\text{CR}}/\text{SiO}_2$: The impregnated and dried $\text{Ni}(\text{NO}_3)_2/\text{SiO}_2$ was calcined at 450 °C for 4 h and then reduced in H_2 flow. The other steps were the same as those for $\text{Ni}_{\text{DR}}/\text{SiO}_2$. Before reduction, the calcined (C) catalyst was denoted as $\text{Ni}_{\text{C}}/\text{SiO}_2$.

3.2. Catalyst Characterization

The specific surface area and pore structure of support and catalyst were determined by N_2 adsorption with a Quadrasorb SI instrument. The crystalline phase of the catalysts was characterized by a Bruker Advance D8 X-ray diffractometer with a $\text{Cu K}\alpha$ radiation source. The H_2 uptake of the catalysts was determined by H_2 chemisorption on a Quantachrome ChemBET Pulsar TPR/TPD instrument. The active Ni area was calculated assuming $\text{H}/\text{Ni}_{\text{surface}} = 1$ and a surface area of $6.5 \times 10^{-20} \text{ m}^2$ per Ni atom. A JEM-2010 transmission electron microscope was employed to examine the Ni particle size of catalysts. Some product samples were analyzed by mass spectrometry (MS model: Q Exactive) to identify the relative amount of condensation byproducts.

3.3. Catalytic Reaction

The hydrogenation of ADN was carried out in a stainless-steel autoclave equipped with a temperature control system and magnetic stirrer. Typically, 5 g ADN (98%, Alfa Aesar, Haverhill, MA, USA), 80 mL of methanol (>99.5%, Beijing Chemical Works, Beijing, China), 5 g pre-reduced catalyst and 0.1 g NaOH (>96.0%, Beijing Chemical Works) were added into the reactor. The hydrogenation conditions were: 80 °C, 3 MPa, 500 rpm. The products were sampled online and analyzed by a gas chromatograph (GC 7890F, Techcomp Instrument Company, Kwai Chung, Hong Kong) equipped with a flame ionization detector and a KB-624 capillary column (30 m \times 0.32 mm \times 1.8 μm , Kromat). The condensation byproducts were high molecular weight secondary and tertiary amines which were not eluted in the GC. Phenylamine was used as the internal standard to determine the content of ADN, ACN, HMD and HMI. The catalytic activity, the conversion of ADN and the selectivity to ACN and HMD were calculated as:

$$\text{Catalytic Activity} = \frac{\text{moles of converted ADN}}{\text{Time} \times m_{\text{Cat}}} \quad (1)$$

$$\text{ADN Conversion} = \frac{\text{moles of converted ADN}}{\text{moles of ADN feedstock}} \times 100\% \quad (2)$$

$$\text{ACN Selectivity} = \frac{\text{moles of ACN}}{\text{moles of converted ADN}} \times 100\% \quad (3)$$

$$\text{HMD Selectivity} = \frac{\text{moles of HMD}}{\text{moles of converted ADN}} \times 100\% \quad (4)$$

4. Conclusions

Supported Ni catalysts for the liquid phase hydrogenation of ADN were investigated. The following conclusions are based on the results and discussion:

1. The support affects the catalytic performance of supported Ni catalysts by providing original acid sites, which promote the condensation side reactions and decrease the selectivity to primary amines. SiO_2 is chosen as the support in this work providing less original acid sites.
2. The catalyst prepared by the direct reaction method, without a prior calcination step, gave smaller Ni particles, this is, a higher Ni dispersion and H_2 uptake capacity, which improved the catalytic activity and inhibited the intermolecular condensation side reaction.

3. The reduction temperature had an appreciable effect on the catalytic performance of Ni_{DR}/SiO₂. 450 °C was regarded as a preferable temperature to suppress the intramolecular condensation reaction to HMI.
4. The addition of NaOH into the reaction system improved the hydrogenation activity and significantly improved the target products selectivity. When the NaOH/Ni mass ratio was increased to 0.5, the selectivity to primary amines attained 94%.

Author Contributions: M.H., Z.J. and C.W. conceived and designed the experiments; Z.J. and C.W. performed the experiments; Z.J. and C.W. analyzed the data; B.Z. and C.W. wrote the paper.

Conflicts of Interest: The authors declare no conflict of interest.

References

1. Dahlhoff, G.; Niederer, J.P.M.; Hoelderich, W.F. Epsilon-Caprolactam: New by-product free synthesis routes. *Catal. Rev. Sci. Eng.* **2001**, *43*, 381–441. [[CrossRef](#)]
2. Tolman, C.A.; Mckinney, R.J.; Seidel, W.C.; Druliner, J.D.; Stevens, W.R. Homogeneous Nickel-Catalyzed Olefin Hydrocyanation. *Adv. Catal.* **1985**, *33*, 1–46. [[CrossRef](#)]
3. Brunelle, J.; Seigneurin, A.; Sever, L. Method for Cyclizing Hydrolysis of an Aminonitrile Compound into Lactam. U.S. Patent 6479658B1, 12 November 2002.
4. Leconte, P. Process for Preparing Lactams. U.S. Patent 20120095212A1, 19 April 2012.
5. Ziemecki, S.B. Selective Low Pressure Hydrogenation of a Dinitrile to an Aminonitrile. U.S. Patent 5151543A, 29 September 1992.
6. Boschhat, V.; Brunelle, J.P.; Darrier, B.; Chevaljer, B.; Bobet, J.L. Hemihydrogenation Method for Dinitriles. U.S. Patent 6521779B1, 18 February 2003.
7. Ziemecki, S.B.; Ionkin, A.S. Aminonitrile Production. U.S. Patent 6080884A, 27 June 2000.
8. Liao, H.; Liu, S.; Hao, F.; Liu, P.; You, K.; Liu, D.; Luo, H. Liquid phase hydrogenation of adiponitrile to 6-aminocapronitrile and hexamethylenediamine over potassium doped Ni/ α -Al₂O₃ catalyst. *React. Kinet. Mech. Catal.* **2013**, *109*, 475–488. [[CrossRef](#)]
9. Chen, B.; Dingerdissen, U.; Krauter, J.G.E.; Rotgerink, H.G.J.L.; Mobus, K.; Ostgard, D.J.; Panster, P.; Riermeier, T.H.; Seebald, S.; Tacke, T. New developments in hydrogenation catalysis particularly in synthesis of fine and intermediate chemicals. *Appl. Catal. A Gen.* **2005**, *280*, 17–46. [[CrossRef](#)]
10. Tichit, D.; Durand, R.; Rolland, A.; Coq, B.; Lopez, J.; Marion, P. Selective half-hydrogenation of adiponitrile to aminocapronitrile on Ni-based catalysts elaborated from lamellar double hydroxide precursors. *J. Catal.* **2002**, *211*, 511–520. [[CrossRef](#)]
11. Hoffer, B.W.; Moulijn, J.A. Hydrogenation of dinitriles on Raney-type Ni catalysts: Kinetic and mechanistic aspects. *Appl. Catal. A Gen.* **2009**, *352*, 193–201. [[CrossRef](#)]
12. Jia, Z.; Zhen, B.; Han, M.; Wang, C. Liquid phase hydrogenation of adiponitrile over directly reduced Ni/SiO₂ catalyst. *Catal. Commun.* **2016**, *73*, 80–83. [[CrossRef](#)]
13. Verhaak, M.J.F.M. The selective hydrogenation of acetonitrile on supported nickel-catalysts. *Catal. Lett.* **1994**, *26*, 37–53. [[CrossRef](#)]
14. Nakagawa, Y.; Nakazawa, H.; Watanabe, H.; Tomishige, K. Total Hydrogenation of Furfural over a Silica-Supported Nickel Catalyst Prepared by the Reduction of a Nickel Nitrate Precursor. *ChemCatChem* **2012**, *4*, 1791–1797. [[CrossRef](#)]
15. Li, H.X.; Xu, Y.P.; Li, H.; Deng, J.F. Gas-phase hydrogenation of adiponitrile with high selectivity to primary amine over supported Ni-B amorphous catalysts. *Appl. Catal. A Gen.* **2001**, *216*, 51–58. [[CrossRef](#)]
16. Louis, C.; Cheng, Z.; Che, M. Characterization of Ni/SiO₂ catalysts during impregnation and future thermal activation treatment leading to metal particles. *J. Phys. Chem.* **1993**, *97*, 5703–5712. [[CrossRef](#)]
17. Braun, J.V.; Blessing, G.; Zobel, F. Katalytische Hydrierungen unter Druck bei Gegenwart von Nickelsalzen, VI: Nitrile. *Berichte der Deutschen Chemischen Gesellschaft (A B Ser.)* **1923**, *56*, 1988–2001. [[CrossRef](#)]
18. Sanchez, K.M. Preparation of 6-Aminocapronitrile. U.S. Patent 5296628A, 22 March 1994.

19. Huang, Y.Y.; Adeeva, V.; Sachtler, W.M.H. Stability of supported transition metal catalysts in the hydrogenation of nitriles. *Appl. Catal. A Gen.* **1991**, *182*, 365–378. [[CrossRef](#)]
20. Ballardur, V.; Fouilloux, P.; deBellefon, C. Monometallic Ni, Co and Ru, and bimetallic NiCr, NiTi and CoFe Ziegler-Sloan-Laporte catalysts for the hydrogenation of adiponitrile into hexamethylenediamine: Effect of water and dopants. *Appl. Catal. A Gen.* **1995**, *133*, 367–376. [[CrossRef](#)]

Sample Availability: Samples of the compounds are available from the authors.



© 2018 by the authors. Licensee MDPI, Basel, Switzerland. This article is an open access article distributed under the terms and conditions of the Creative Commons Attribution (CC BY) license (<http://creativecommons.org/licenses/by/4.0/>).